NASA TECHNICAL MEMORANDUM

NASA TM X-52298

NASA TM X-52298

SUMMARY OF NASA RADIAL TURBINE RESEARCH RELATED TO BRAYTON CYCLE SPACE POWER SYSTEMS

by H. E. Rohlik, M. G. Kofskey, and T. Katsanis

Lewis Research Center
Cleveland, Ohio

TECHNICAL PAPER proposed for presentation at Second Interagency Energy Conversion Engineering Conference, Miami Beach, Florida, August 13-17, 1967

NATIONAL AERONAUTICS AND SPACE ADMINISTRATION · WASHINGTON, D.C. · 1967

SUMMARY OF NASA RADIAL TURBINE RESEARCH RELATED TO BRAYTON CYCLE SPACE POWER SYSTEMS

by H. E. Rohlik, M. G. Kofskey, and T. Katsanis

Lewis Research Center
Cleveland, Ohio

TECHNICAL PAPER proposed for presentation at
Second Interagency Energy Conversion Engineering Conference
Miami Beach, Florida, August 13-17, 1967

NATIONAL AERONAUTICS AND SPACE ADMINISTRATION

SUMMARY OF NASA RADIAL TURBINE RESEARCH RELATED TO BRAYTON CYCLE SPACE POWER SYSTEMS

by H. E. Rohlik, M. G. Kofskey, and T. Katsanis

Lewis Research Center

National Aeronautics and Space Administration

Cleveland, Ohio

E-3940

ABSTRACT

Progress to data at the Lewis Research Center is reported in two areas, new techniques for turbine analysis and experimental investigations of turbine performance. Radial-flow turbines were investigated for effects of size, Reynolds number, and specific speed on efficiency and flow. Results indicate that turbines for wide ranges of operating variables may be designed with a reasonable certainty of achieving high efficiency.

Thirteen NASA publications are listed.

INTRODUCTION

Interest in Brayton Cycle space power systems resulted in a technology programs at the Lewis Research Center, beginning in 1962. To date, this program has included cycle studies, system operation studies, and component investigations. References 1 and 2 examine cycle variables, such as temperature, pressure, and component efficiency, for their effects on system performance. These studies led to the selection of optimum temperature and pressure ratios from the standpoint of system size relative to electrical output. Subsequently, a reference two-shaft 10-kilowatt system was established to define individual components for further study. In this system, the turbine-compressor shaft rotates at a much higher rate than the turboalternator shaft. References 3 and 4 describe analog and experimental operation of closed-loop systems.

The third technology area has included the development of some new analytical techniques for turbine design as well as extensive experimental investigations of turbomachinery designed for the reference 10-kilowatt system. The objectives of this effort included the improvement of component performance and the determination of component size and type best suited to various applications. A 6.02-inch radial turbine was designed to drive the compressor of the reference system. This size resulted from consideration of system pressure and its influence on size and performance of the various heat-transfer and rotating components. Two scale models were built to examine the effects of scaling and Reynolds number. Other hardware included a centrifugal compressor.

This paper reviews the analytical turbine work and the major results of the experimental turbine programs.

NOMENCLATURE

A	constant
B	constant
D_1	turbine-rotor-inlet-tip diameter
D_2	turbine-exit mean diameter
H	isentropic specific work based on total-pressure ratio, (ft)(lb)/lb
h	turbine blade height
Δh_{id}	ideal turbine work based on inlet total pressure and exit static pressure
$\Delta h'_{id}$	ideal turbine work based on inlet total pressure and exit total pressure
N	turbine rotative speed, rpm
N_s	specific speed, $(N\sqrt{Q})/H^{3/4}$, rpm $ft^{3/4}/sec^{1/2}$
Q	volume flow (based on exit conditions), ft^3/sec
R	Reynolds number, $w/\mu r_t$
r_t	rotor tip radius, ft
u	turbine-exit mean-blade speed
V_x	meridional absolute gas velocity
w	mass flow rate, lb/sec
α	stator-exit flow angle, degrees from meridional plane
η_s	static efficiency (based on total- to static-pressure ratio across turbine)
η_t	total efficiency (based on total- to total-pressure ratio across turbine)
μ	dynamic gas viscosity (based on inlet conditions), lb/(ft)(sec)
ν	blade-jet speed ratio (based on rotor inlet tip speed)

Subscripts:

ref	reference

REFERENCE SYSTEM

Studies of cycle performance led to the selection of optimum temperature and pressure ratios and levels in view of current technology limits in materials and component performance. These conditions were then used to establish a reference power-generation system upon which experimental programs could be based. Figure 1 shows a schematic diagram of the reference system used for component investigations to date. It is a two-shaft solar-powered unit with argon as the working fluid. The turbine pressure ratios are 1.56 for the compressor-drive unit and 1.26 for the alternator-drive unit, and the compressor ratio is 2.3. The cycle output is 10 kilowatts in shaft power to the alternator.

Considerations of turbomachinery size and heat-transfer component effectiveness led to a compressor inlet pressure of 6.0 psia.

Turbomachinery efficiencies were varied in the cycle studies so that their influence on cycle performance could be evaluated. The significance of component efficiency in the reference system is shown in figure 2, where cycle efficiency is presented as a function of compressor efficiency and overall turbine efficiency. Note that three points in turbine efficiency correspond to about three points in cycle efficiency. With cycle efficiencies in the 0.25 range, this makes 1 point in turbine efficiency equivalent to 4 percent in net power output. The significance of compressor efficiency is comparable.

Reference 5 describes the manner in which turbomachinery components may be selected for given operating characteristics. This approach was used in the subject programs. Turbomachinery designed for the reference system is shown in figure 3. The radial turbocompressor (fig. 3) employs components of 6-inch diameter.

ANALYTICAL DESIGN TECHNIQUES

Design Geometry of Radial Turbines

Radial turbines have performance and design features that make them suitable for a variety of applications. Since the form of a radial turbine varies greatly for various applications, it is desirable to have a correlation between the design features and turbine losses. The literature provides some of this information. A further study of turbine losses as affected by turbine geometry was made in order to facilitate the selection of such parameters as inlet- to exit-diameter ratio and stator angle, in optimum combination for any given application.

Specific speed has been used to characterize axial and radial turbines according to application by relating speed, work, and flow. The usual form of the relation $N_s = (N\sqrt{Q})/(H^{3/4})$ provides a rather gross relation that may be expanded to include a number of specific velocity diagram and geometry parameters. The expanded equation may be expressed as follows:

$$N_s = \text{constant} \left(\frac{\Delta h_{id}}{\Delta h'_{id}}\right)^{3/4} \nu^{3/2} \left(\frac{V_x}{u}\right)_2^{3/4} \left(\frac{D_2}{D_1}\right)^{3/2} \left(\frac{h}{D}\right)_2^{1/2} \qquad (1)$$

This equation makes it clear that any given specific speed value can be achieved by an infinite number of combinations of the aforementioned ratios and with a corresponding variety of efficiency levels. The problem, therefore, is to find the combination at each specific speed that will result in maximum efficiency.

Losses calculated in this analysis were in stator-blade-row boundary layers, rotor-passage boundary layers, blade-shroud clearance, disc windage, and exit velocity. Turbine performance was then calculated for a fixed-blade-tip critical velocity of 0.49 and for wide ranges of the following independent variables: stator-exit flow angle (52° to 84°), ratio of stator blade height to rotor tip diameter (0.007 to 0.408), and rotor-exit to rotor-inlet diameter ratio (0.175 to 0.6). These quantities result in a variety of combinations of the variables listed in equation (1). Several assumptions concerning rotor reaction, tip-diameter ratio, and exit-hub to tip-diameter ratio, and other items were required to define internal velocities and limit the calculated configurations to reasonable geometric shapes.

Results of the analysis were evaluated in terms of efficiency and specific speed, as shown in figure 4. The lower curve envelopes all the calculated combinations of the independent variables and is therefore the curve of maximum static efficiency for the specific efficiency for the specific speed range shown. It might be noted that, in the intermediate specific speed range, static efficiency varied by as much as fifty points at a fixed value of specific speed.

The curve of total efficiency corresponds to the curve of maximum static efficiency. The large difference between total and static efficiencies at high values of specific speed corresponds to turbine exit mach numbers up to 0.6. This curve of static efficiency is also the curve of optimum geometry. Calculated points on and near the curve were examined and plotted in terms of the geometric characteristics. One such plot is presented in figure 5, where optimum stator angle is shown as a function of specific speed. Optimum stator-exit flow angle shows a continuous variation with specific speed, ranging from 83° at a specific speed of 20 down to 56° at a specific speed of 174.

Figure 6 shows sections of turbines with a geometry corresponding to the maximum static-efficiency curve at three values of specific speed. The exit-hub tip-diameter ratio was 0.4 for all optimum configurations, while all other geometric characteristics varied with specific speed.

The distribution of calculated loss along the maximum static-efficiency curve is shown in figure 7, which shows trends in internal flow with varying specific speed. The lower values of specific speed reflect low-volume flow rates relative to turbine size, so all losses except exit velocity become larger to specific work as specific speed decrease. This results from the increased area of the surfaces generating losses relative to the flow area. Large-volume flows at the high values of specific speed make the exit loss predominant.

Internal Velocity Calculations

Quasi-three-dimensional methods have been developed and used for analyzing flow through mixed-flow turbomachines. The first step in these methods is to obtain a two-dimensional solution on an assumed mean stream surface between the blade (see fig. 8(b)). This two-dimensional solution is based on an equation for the velocity gradient along the normal to the projection of the streamlines on a plane containing the axis of rotation (fig. 9). This plane is called the meridional plane, and the projections of the streamlines are called meridional streamlines. The streamlines and their normals are used to establish a grid for a meridional-plane solution. In cases where the distance between the hub and shroud is great and there is a large change in flow direction within the rotor, the normals vary considerably in length and direction during the course of the calculations. Therefore, it becomes difficult to obtain a direct solution on the computer without resorting to intermediate graphical steps.

The use of normals is not essential to the method, and it is possible to obtain a direct solution by the use of a set of arbitrary curves from hub to shroud

instead of streamline normals (ref. 6). These arbitrary curves are termed quasi-orthogonals. The quasi-orthogonals are not necessarily orthogonal to each streamline but merely intersect every streamline once across the width of the passage. The quasi-orthogonals remain fixed regardless of any change of streamlines. By using this technique, it was possible to develop a computer program that calculates a streamline solution in the meridional plane without any intermediate graphical procedures even for turbomachines with wide passages and a change in direction from radial to axial within the rotor blade. The basic idea used to obtain a meridional solution using quasi-orthogonals can be applied to obtain a blade-to-blade solution (ref. 7). In this case, the quasi-orthogonals run from blade-to blade on a stream surface determined by the meridional solution.

The basic assumptions are that there is steady relative flow, and that the flow is nonviscous and isentropic. To this a correction for losses is made by assuming a loss in relative total pressure that varies from zero at the inlet to a maximum at the outlet of the blade passage. Typical hub-to-shroud and blade-to-blade surfaces are shown in figure 8(a) for a straight blade turbine.

The initial assumption used is that the mean surface between the blades is a stream surface. With this assumption, a two-dimensional meridional-plane solution can be obtained. This solution defines a blade-to-blade surface for each meridional streamline, and then solutions are obtained on these surfaces, giving a velocity distribution throughout the passage.

The key to the method is the velocity gradient equation, which is an equation for the directional derivative of the relative velocity along a given quasi-orthogonal on a surface (hub-to-shroud, blade-to-blade, or other). The velocity gradient is a function of the relative velocity, and streamline geometry. To evaluate the parameters involved, an initial streamline geometry must be established. For this, fixed curves between flow boundaries are specified on the assumed stream surfaces, at several stations from inlet to outlet (for either a hub-to-shroud or a blade-to-blade stream surface). These curves are the quasi-orthogonals along which the velocity gradient equation will be integrated. For an initial approximation to the streamlines, each quasi-orthogonal can be divided into a number of equal spaces. The quasi-orthogonals and initial streamline assumptions are shown in figure 9 for a hub-to-shroud stream surface of a radial inlet gas turbine with splitter blades. The success of the method is based on the fact that, for a reasonable assumed streamline pattern, the geometrical streamline parameters involved are not too different from those of the final solution. Along any quasi-orthogonal, interpolation can be used to determine the streamline spacing that will give equal weight flow between any two adjacent streamlines. When this is done for every quasi-orthogonal from inlet to outlet, a new estimate for the streamline pattern is obtained, and the geometry parameters in the velocity gradient equation can be determined more accurately. Repeating the process, one can obtain a solution for the velocities along each quasi-orthogonal. The meridional streamline solution for a radial turbine is shown in figure 10. This solution is followed by a blade-to-blade analysis made at hub, mean, and shroud streamlines with the use of the quasi-orthogonal techniques again.

Figure 11 shows the blade loading on main and splitter blades at the hub, mean, and shroud obtained by this method for a radial inflow turbine. This type of analysis could be very useful as a design tool, since it points out the location of possible flow separation. Modifications can be made in the geometry to improve on the velocity distributions until a good design is evolved.

Off-Design Performance Estimation

Techniques for the estimation of axial performance have been available for many years and have proven quite useful in turbine design. Radial turbines may be examined in the same general manner. The change in radius through the machine, however, requires special consideration in the gap between stator and rotor and through the rotor. A method for estimating off-design performance with a given set of reference-point operating conditions is described in reference 8. Loss coefficients were calculated to make the calculated performance agree with the reference efficiency and operating conditions, and then these loss coefficients were used as constants over wide ranges of speed and pressure ratio. Figure 12 shows experimental points and calculated curves of specific work as a function of speed and pressure ratio. Good agreement between calculation and experiment is shown. Weight-flow calculations showed agreement within 4 percent at all but the very low-pressure ratios, which indicated the need for a refinement in the estimation procedure. The method described in reference 8 assumed zero rotor-entrance loss when the relative inlet-velocity vector was radial. A modification is underway to calculate to an optimum relative-inlet-gas angle in a manner similar to that used for the determination of the centrifugal compressor "slip factor". Zero inlet loss will then occur at the optimum inlet angle with incidence loss increasing with deviation from the optimum angle. This modification is expected to improve the accuracy of the off-design performance estimation

EXPERIMENTAL INVESTIGATIONS

Test Facility

The apparatus used in the performance evaluation of the turbines to be discussed is shown in figure 13. Argon, from a high-pressure supply system, was heated, filtered, and then passed through a mass-flow measuring station that consisted of a calibrated flat-plate orifice. A pressure control valve upstream of the turbine regulated the turbine-inlet pressure. With a fixed inlet pressure, a remotely controlled valve in the low-pressure exhaust line was used to maintain the desired pressure ratio across the turbine. The power output of the turbine was absorbed and the speed controlled by an air-brake dynamometer that was cradle mounted on air bearings for torque measurement.

Description of Research Turbines

A photograph of the radial compressor-drive turbine rotor and scroll-stator assembly is presented in figure 14. The 6.02-inch-tip-diameter rotor has 11 blades and 11 splitter blades. These splitter blades extend over approximately one-third the length of the blade from the leading edge and thereby decrease the blade loading in that region and prevent low velocities on the pressure surface at the hub. The stator assembly consists of 14 stator blades, one of which has an extended leading edge portion to block the flow from entering the small end of the scroll and prevent recirculation of the working fluid. A 0.762-scale version

of this turbine, 4.59-inch-tip diameter, was also tested and the results reported in reference 9. Although it was intended that the 4.59-inch-tip-diameter turbine be geometrically similar to the 6.02-inch turbine, some differences existed in the test units. One of these differences was the shroud-clearance values, which could have an effect on performance. The rotor-axial and exducer-radial shroud clearances, when expressed as a percentage of blade height, were 1.9 and 1.4 percent, respectively, for the 4.59-inch turbine. The corresponding axial and radial shroud clearances for the 6.02-inch turbine were 2.5 and 0.7 percent, respectively.

Performance Evaluation

The attainment of high turbine performance is demonstrated by the results of the experimental cold-argon investigation of the 6.02-inch radial turbine as reported in reference 10. Total and static efficiencies are shown in figure 15 as a function of blade-jet speed ratio. This data was obtained in cold tests at a Reynolds number $Re = (w/\mu r_t)$ of 225 000 which is approximately 3.5 times higher than the design value of 63 700 for hot operation at design speed and pressure ratio. The figure shows that total and static efficiencies of 0.90 and 0.84 were obtained at the design blade-jet speed ratio of 0.697.

Since the design Reynolds number of the turbines under consideration are in the range where performance may deteriorate with a decrease in Reynolds number, the 6.02-inch and the scaled 4.59-inch turbines were investigated over a range of Reynolds number. Results of these investigations are reported in references 11 and 12. Efficiency as a function of Reynolds number at equivalent design speed and pressure ratio is shown in figure 16 for both turbines. This figure, therefore, indicates the effects of changes in Reynolds number and size on performance. Size effects include the effects of such factors as tip clearance, surface finish, and flow-surface deviations due to fabrication or machining. Performance comparison of the turbines at their respective design values of Reynolds number shows that the 4.59-inch turbine is about 2 points lower both in total and static efficiency. As previously noted, shroud clearances when expressed as a percentage of blade height were not the same. The radial shroud clearance for the 4.59-inch turbine was about twice as large as that for the 6.02-inch turbine. Hence, the difference in shroud clearance may have been a major factor effecting the difference in performance levels between the two turbines. Figure 16 shows that, for the 6.02-inch turbine, the total efficiency increased from approximately 0.85 to 0.90 as the corresponding Reynolds number was increased from 20 000 to 225 000. The corresponding static efficiency increased from 0.80 to 0.84.

The performance of the turbine at various Reynolds numbers may be expressed in terms of a loss ratio $(1 - \eta_t)/(1 - \eta_{t,ref})$ where $(1 - \eta_{t,ref})$ is determined at a reference Reynolds number. The variation of this loss ratio with the Reynolds number ratio Re/Re_{ref} for both turbines is shown in figure 17 with a reference Reynolds number of 225 000. The variation of the loss ratio is approximately the same for the two turbines for the range of Reynolds number over which they are compared.

Since turbulent boundary layer losses are only one of the factors that contribute to overall turbine loss, their relation to Reynolds number cannot be expected to follow the one-fifth power law for turbulent boundary layer losses. However, the relation can be approximated by an equation of the form

$$\frac{1 - \eta_t}{1 - \eta_{t,ref}} = A + B\left(\frac{Re}{Re_{ref}}\right)^{-1/5} \qquad (2)$$

where the values of the constants A and B depend on turbine type and design factors such as rotor blade-tip clearance, surface diffusion, and loading. Figure 17 shows that good agreement is obtained between both turbines and the empirical curve where $A = 0.4$ and $B = 0.6$ for the reference Reynolds number of 225 000. This then indicates that 60 percent of the turbine losses are associated with turbulent boundary layer losses and 40 percent with the other losses.

Effect of Specific Speed on Performance of A Radial Turbine

Reference 13 presents the results of an experimental investigation of the specific speed effect on performance for a particular turbine size with the rotor tip clearance and Reynolds number held constant. Two approaches were considered to achieve the range of specific speeds. One was to design and fabricate an optimized stator and rotor configuration for each specific speed point, and the other was to use several stators with one rotor configuration. The second approach was chosen because it would minimize the time and cost of the program; however, less than optimum turbine configurations resulted, especially at the extremes of the specific speed range.

The 4.59-inch turbine, described previously, was chosen as the research turbine. The design specific speed for this turbine is 95.6. Three additional stators with throat areas nominally 50, 75, and 125 percent of design were also used in the specific speed investigation. Figure 18 shows the four stators and the rotor used in the investigation. These four configuration gave a specific speed range of 68 to 107 at equivalent design speed and pressure ratio.

Figure 19 presents the variation of equivalent weight flow eith stator throat area at equivalent design speed and pressure ratio. Equivalent weight flow is expressed as a percentage of the experimental value obtained with the 100-percent configuration. The dashed line shown in the figure represents the case where equivalent weight flow is directly proportional to stator throat area. Comparison of the experimental curve with the ideal case shows that the weight flow increased at a lower rate than the rate of area increase. This indicates that the stator-exit static to inlet total-pressure ratio increased with increasing stator throat area and, therefore, rotor reaction increased.

Figure 20 shows the variation of total and static efficiency with specific speed for all four configurations investigated. The dashed line represents the variation of efficiency with specific speed at the design blade-jet speed ratio of 0.697. The highest total-efficiency value of 0.91 was obtained at a specific speed of approximately 86. It may be noted that the curve of the design blade-jet speed ratio (dashed line) passes through the peak efficiency point for all but the 50-percent configuration. The heavy curve shown in the figure represents the envelope of the efficiency curves for all configurations. This curve shows that

maximum total efficiency is obtained in the specific speed range of about 80 to 90.

The highest static-efficiency value of 0.87 was also obtained at a specific speed of approximately 86. The lowest peak static efficiency of 0.77 was obtained at a specific speed of 111. It should be pointed out, however, that part of this decrease in static efficiency results from using the same rotor with each stator. Since the 125-percent configuration passes the largest volume flow of the four configurations, the rotor-exit kinetic energy would be expected to be higher for this configuration.

SUMMARY

A Brayton cycle technology program has been underway at the Lewis Research Center since 1962. Major areas of effort include cycle studies, system operation studies, and component investigations. Work in turbines has included analytical and experimental investigations of radial and axial machines. Analytical examinations have been made of radial-turbine design geometry, calculation of internal gas velocities, and the estimation of off-design performance. Computer programs written for these analyses have been developed and are available to the public.

Small radial turbines have demonstrated high efficiencies, 85 to 90 percent, over a large Reynolds number range. The effect of Reynolds number on turbine efficiency can be adequately expressed in a simple relation relating turbine loss to Reynolds number raised to a fractional power. Investigations of turbine size were inconclusive because of disparities in relative blade-shroud clearances in the models tested.

Analytical treatments for radial turbines have been developed in the areas of design geometry selection, calculation of internal gas velocities, and off-design performance estimation.

REFERENCES

1. D. T. Bernatowicz, "NASA Solar Brayton Cycle Studies", presented at the Symposium on Solar Dynamics Systems, Solar and Mechanic Working Groups of the Interagency Advanced Power Group, Washington, September 24-25, 1963.

2. A. G. Glassman, "Computer Program For Thermodynamic Performance of Brayton-Cycle Space-Power Systems", NASA Technical Memo X-1339, January, 1967.

3. H. G. Hurrell and R. L. Thomas, "Control and Start-up Considerations For Two-Spool Solar-Brayton Power System", NASA Technical Memo X-1270, August, 1966.

4. R. Y. Wong, R. C. Evans, and D. J. Spackman, "Preliminary Experimental Evaluation of a Brayton Cycle Turbocompressor Operating on Gas Bearings", NASA Technical Memo X-52261, 1966.

5. M. G. Kofskey and A. J. Glassman, "Turbomachinery Characteristics of Brayton Cycle Space-Power-Generation Systems", ASME Paper No. 64-GTP-23, March, 1964.

6. T. Katsanis, "Use of Arbitrary Quasi-Orthogonals For Calculating Flow Distribution In the Meridional Plane of a Turbomachine", NASA Technical Note D-2546, December, 1964.

7. T. Katsanis, "Use of Arbitrary Quasi-Orthogonals For Calculating Flow Distribution On a Blade-To-Blade Surface In a Turbomachine", NASA Technical Note D-2809, May, 1965.

8. S. M. Futral, Jr., and C. A. Wasserbauer, "Off-Design Performance Prediction With Experimental Verification For a Radial-Inflow Turbine", NASA Technical Note D-2621, February, 1965.

9. C. A. Wasserbauer, M. G. Kofskey, and W. J. Nusbaum, "Cold Performance Evaluation of a 4.59-Inch Radial-Inflow Turbine Designed for a Brayton-Cycle Space Power System", NASA Technical Note D-3260, February, 1966.

10. M. G. Kofskey and D. E. Holeski, "Cold Performance Evaluation of a 6.02-Inch Radial Inflow Turbine Designed For a 10-Kilowatt Shaft Output Brayton Cycle Space Power Generation System", NASA Technical Note D-2987, September, 1965.

11. D. E. Holeski and S. M. Futral, Jr., "Experimental Performance Evaluation of a 6.02-Inch Radial-Inflow Turbine Over a Range of Reynolds Number", NASA Technical Note D-3824, January, 1967.

12. W. J. Nusbaum and C. A. Wasserbauer, "Experimental Performance Evaluation of a 4.59-Inch Radial-Inflow Turbine Over a Range of Reynolds Number", NASA Technical Note D-3835, February, 1967.

13. M. G. Kofskey and C. A. Wasserbauer, "Experimental Performance Evaluation of a Radial-Inflow Turbine Over a Range of Specific Speeds", NASA Technical Note D-3742, November, 1966.

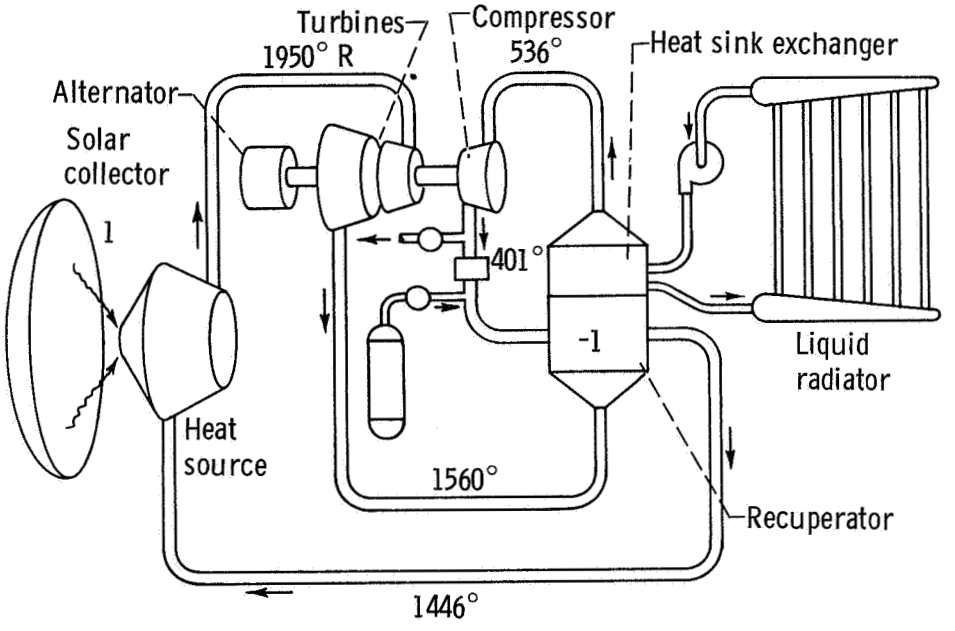

Figure 1. - Schematic diagram of solar Brayton cycle system. Argon used as working fluid.

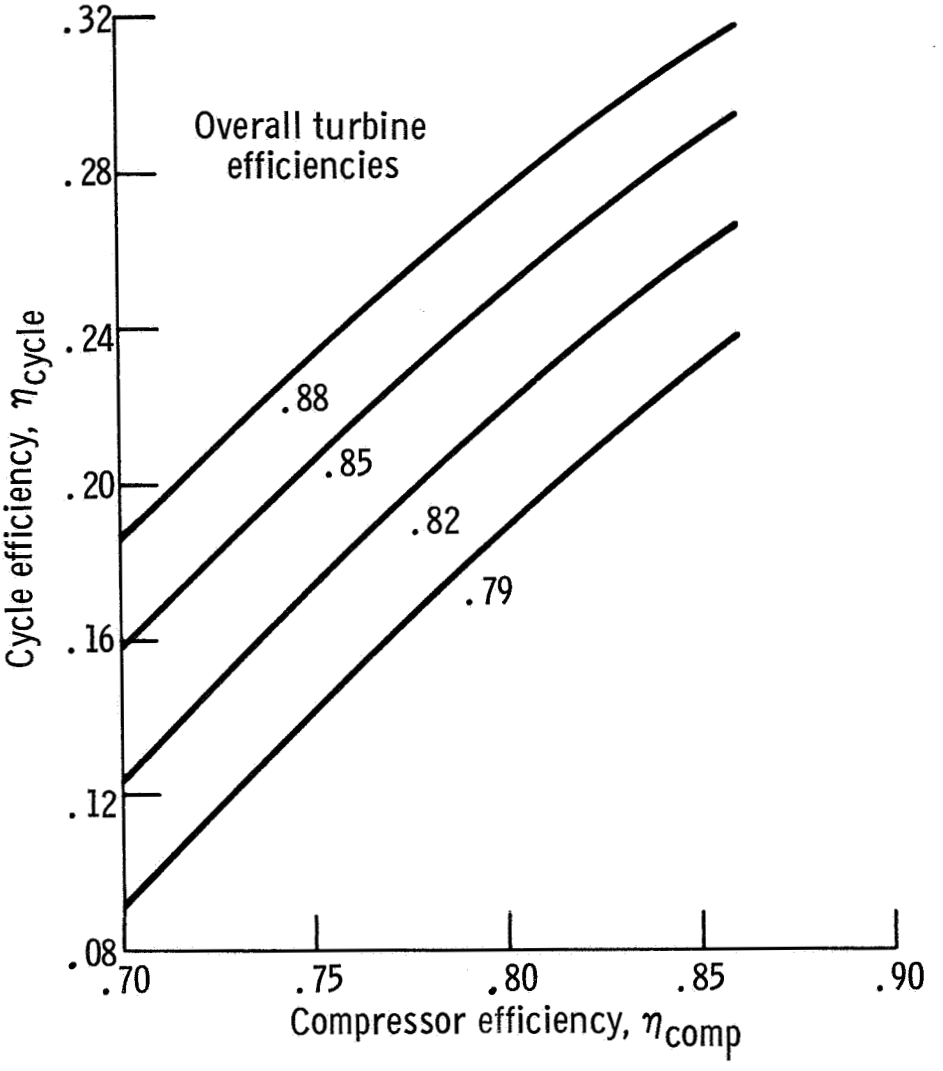

Figure 2. - Effect of turbomachinery efficiency with constant collector area and prime radiator area.

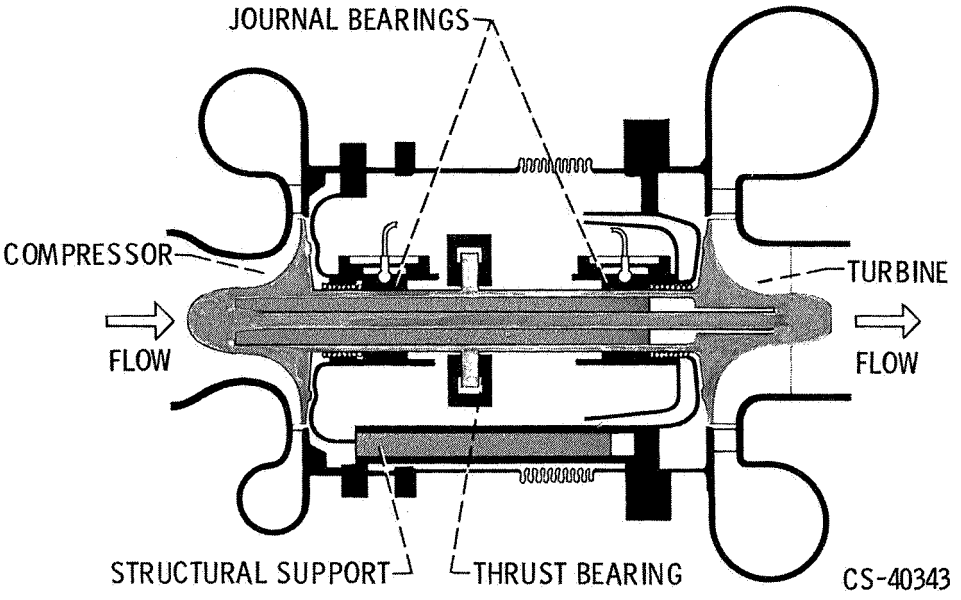

Figure 3. - Schematic diagram of radial turbocompressor.

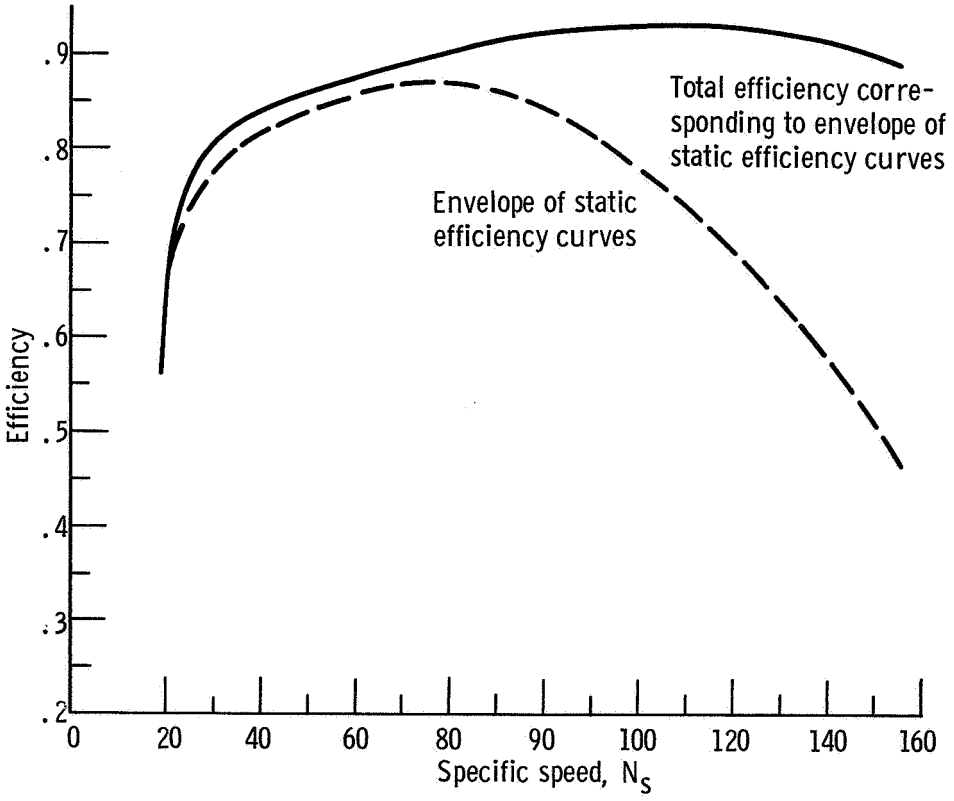

Figure 4. - Range of performance calculated for several stator exit flow angles.

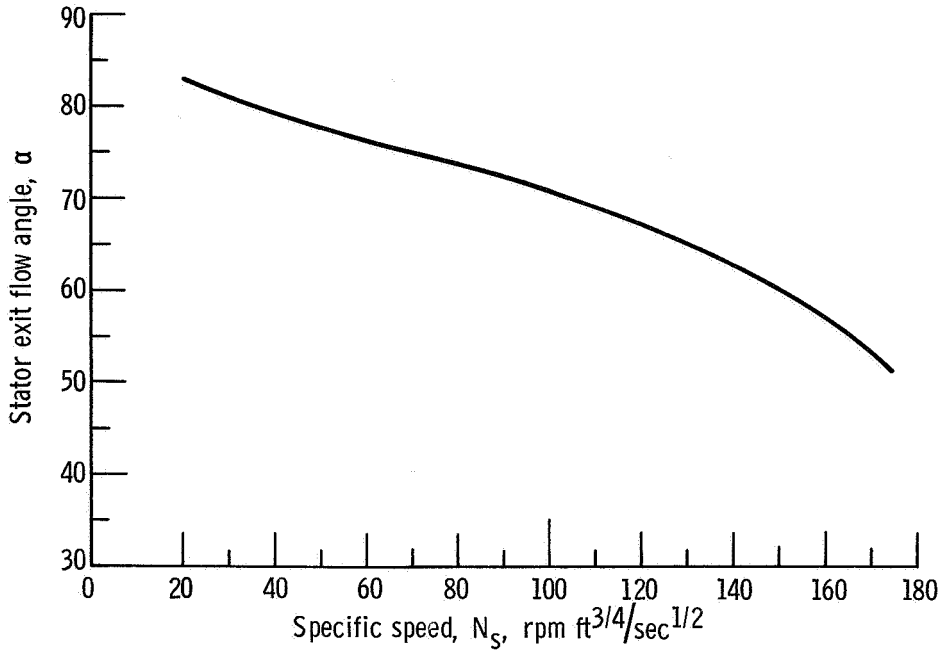

Figure 5. - Variation in optimum stator exit angle with specific speed.

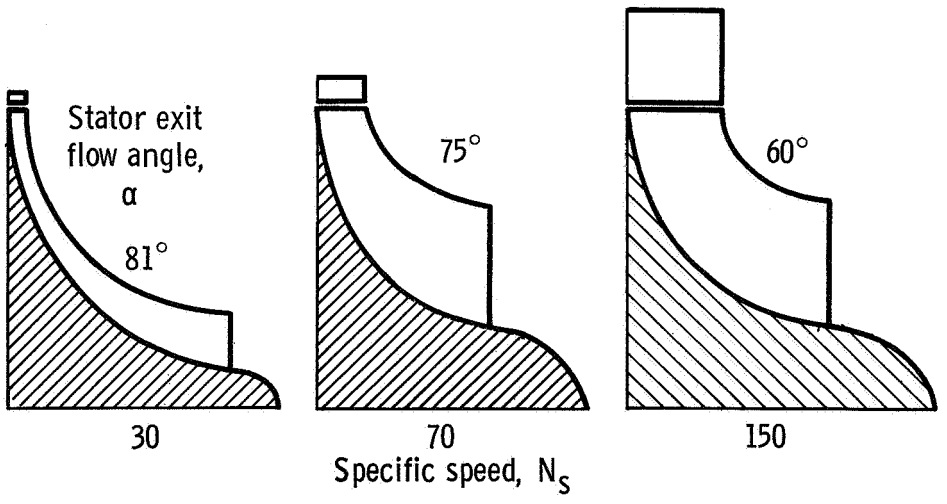

Figure 6. - Sections of radial turbines of minimum calculated loss.

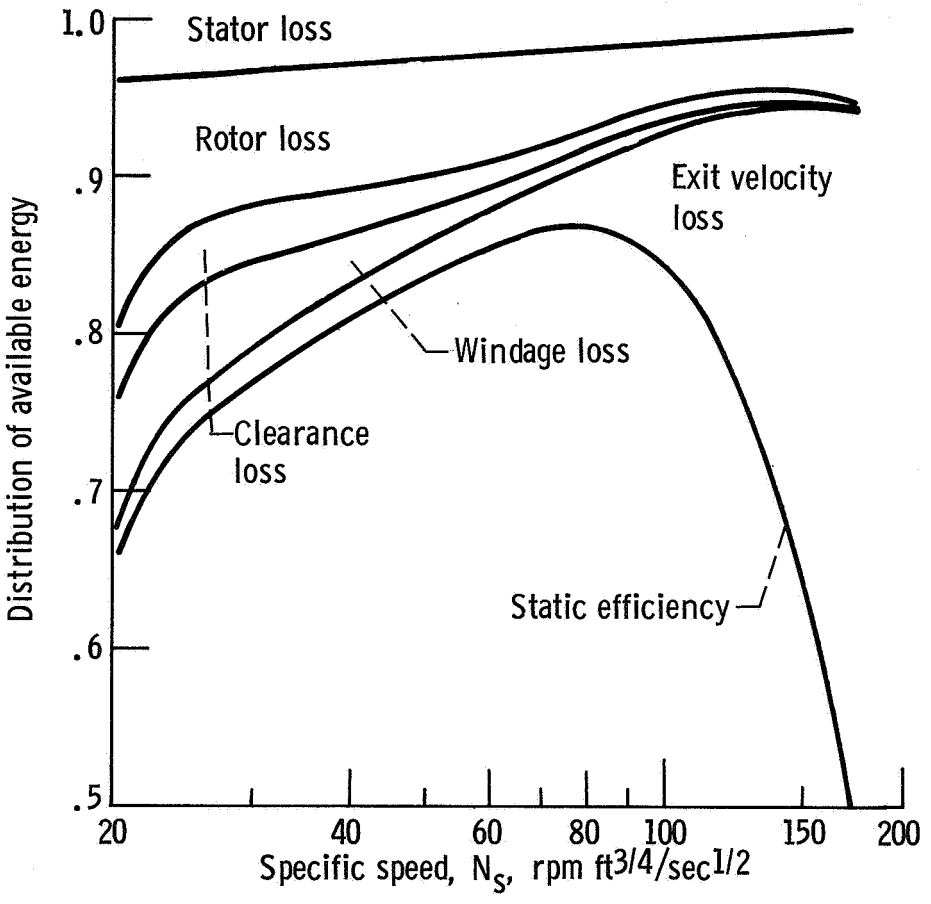

Figure 7. - Loss distribution along curve of maximum total-to-static efficiency.

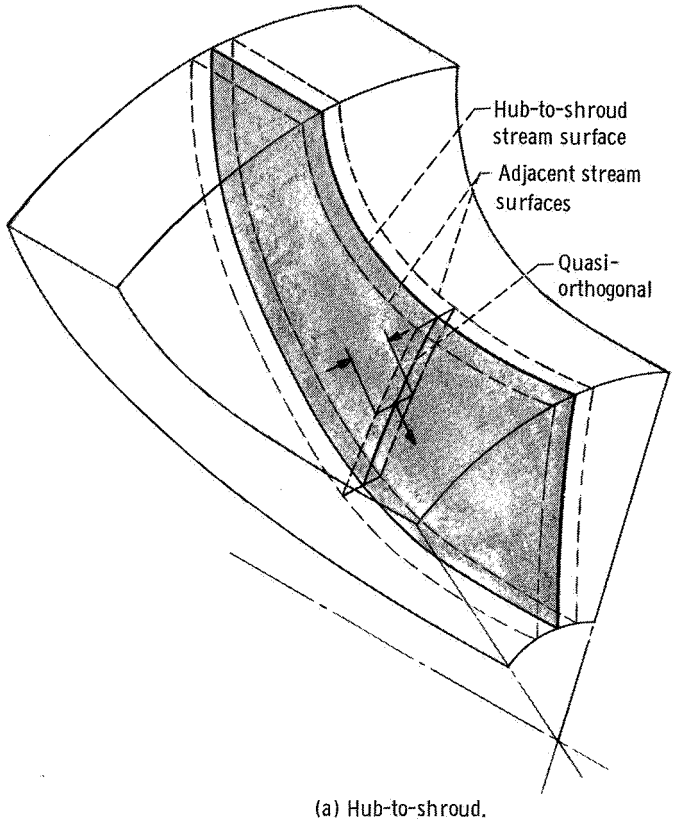

(a) Hub-to-shroud.

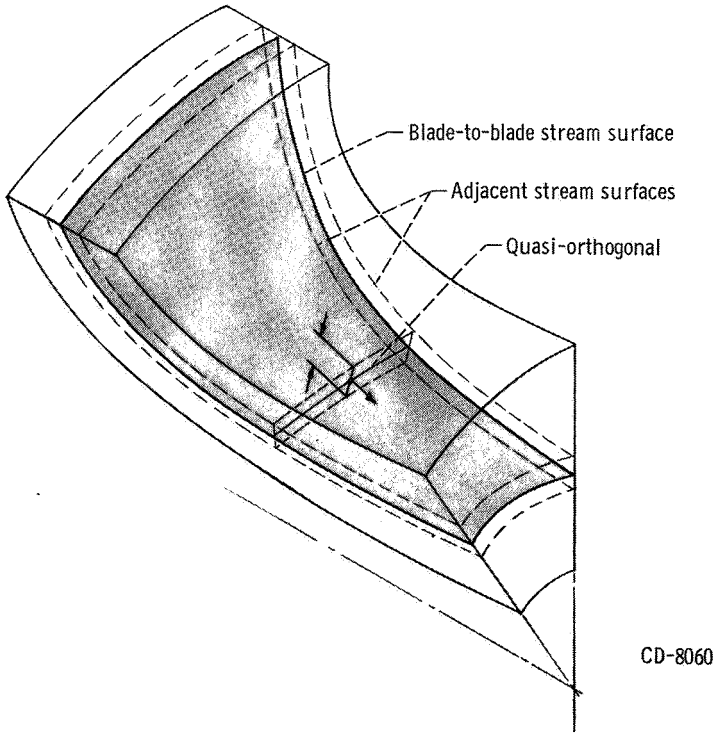

(b) Blade-to-blade.

Figure 8. - Typical stream surfaces in a straight bladed turbine.

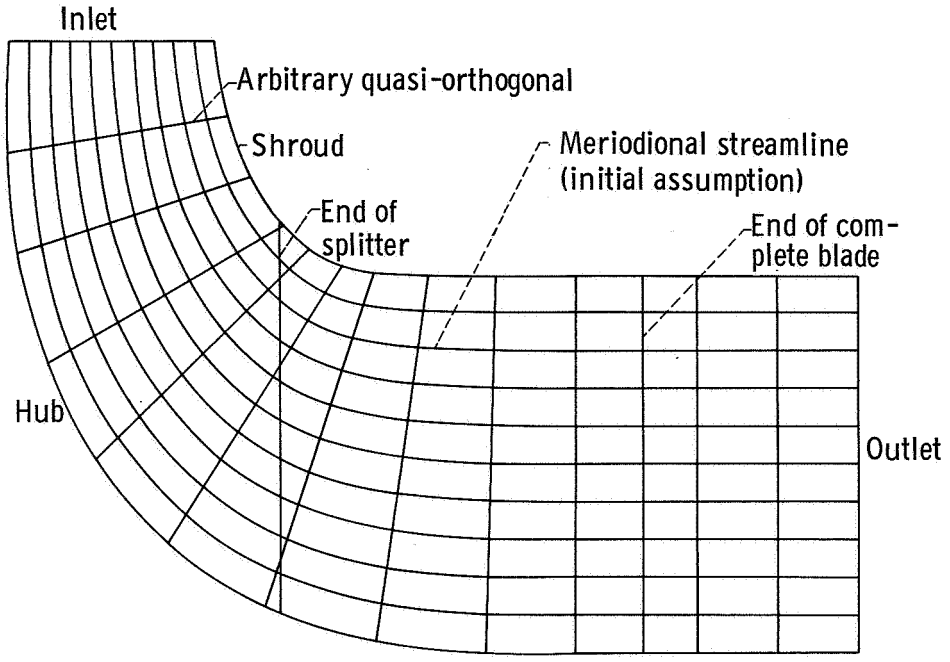

Figure 9. - Hub-shroud profile of rotor in numerical example.

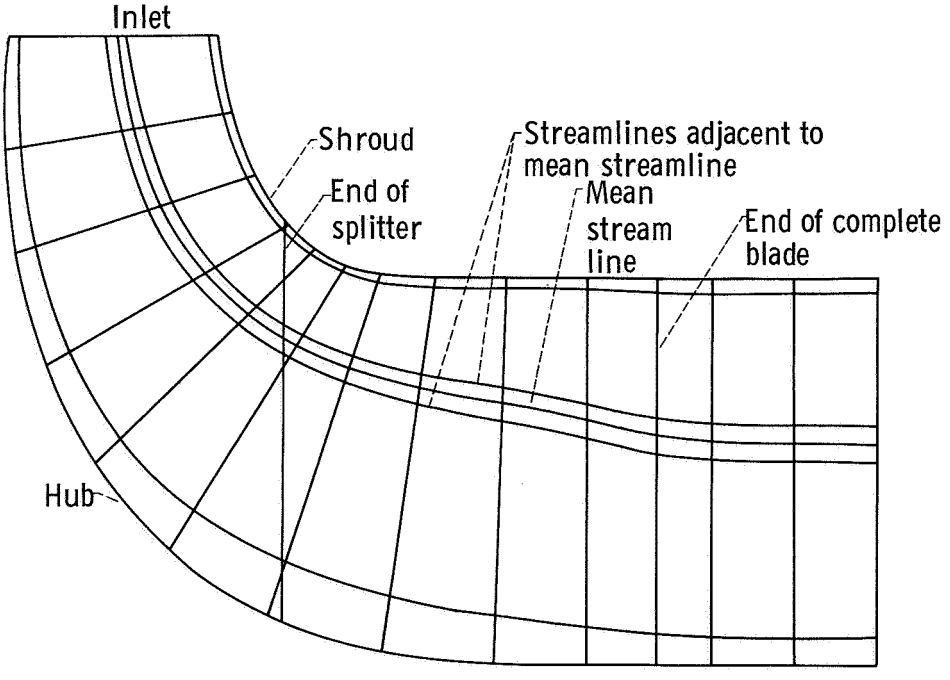

Figure 10. - Hub-shroud profile with streamlines used for blade-to-blade analysis.

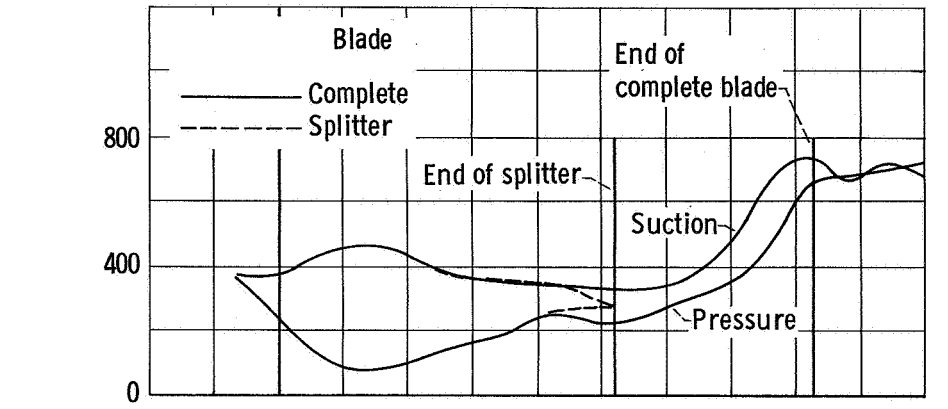

(a) Hub.

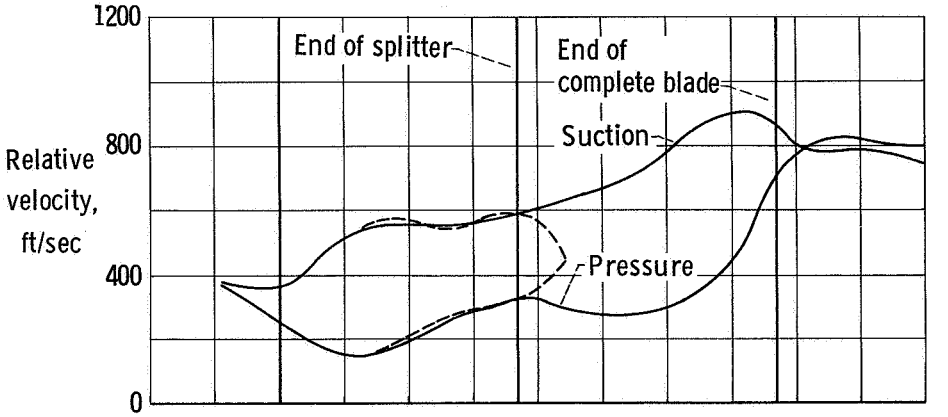

(b) Mean.

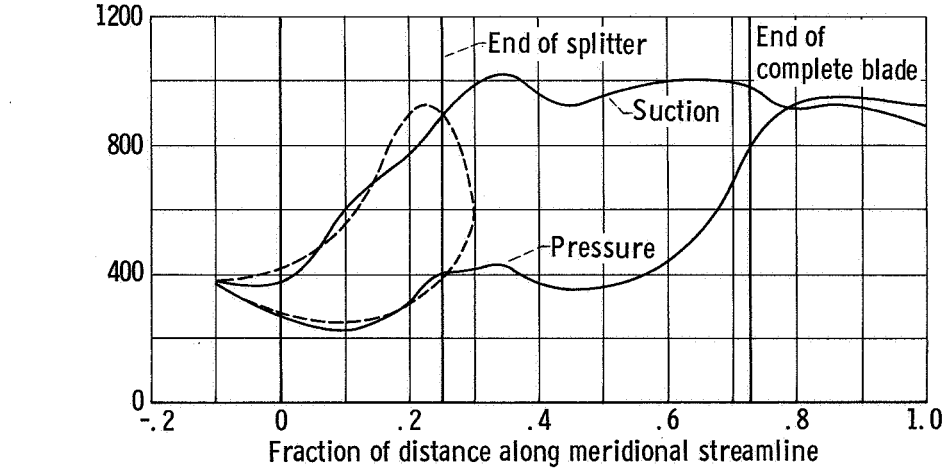

(c) Shroud.

Figure 11. - Blade velocity distribution for numerical example.

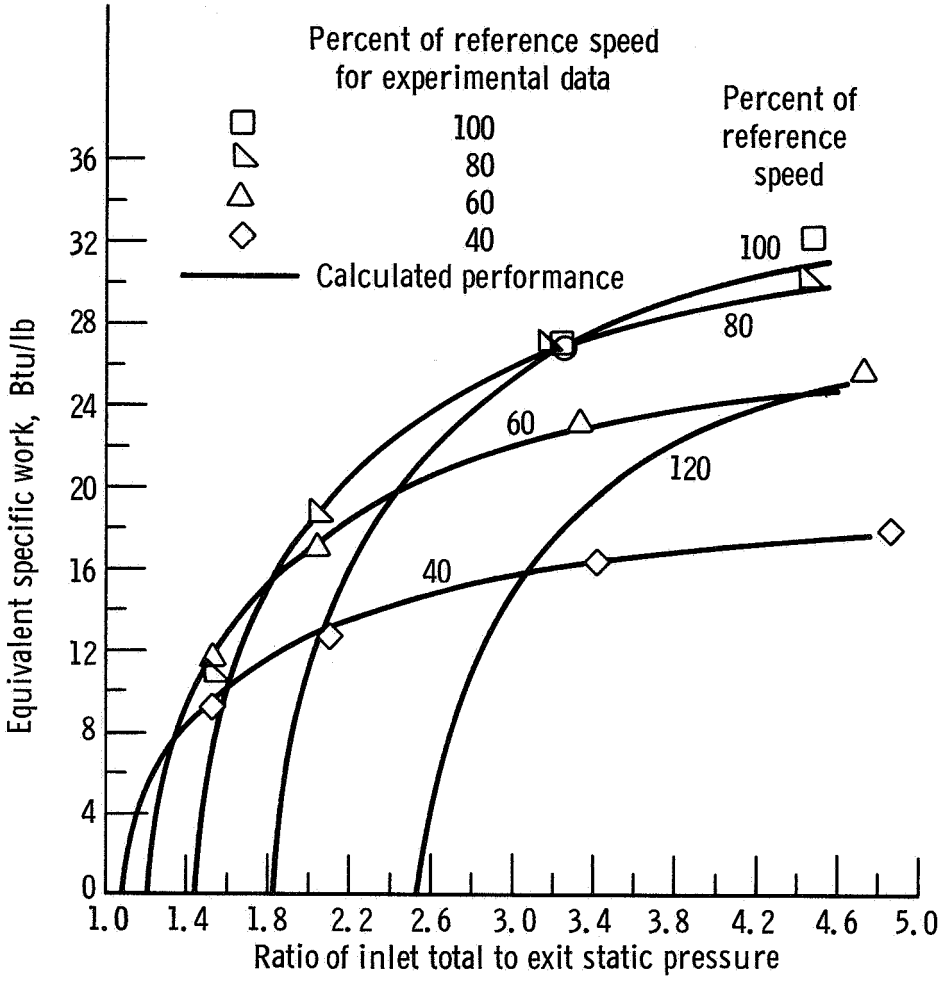

Figure 12. - Variation of equivalent specific work with pressure ratio.

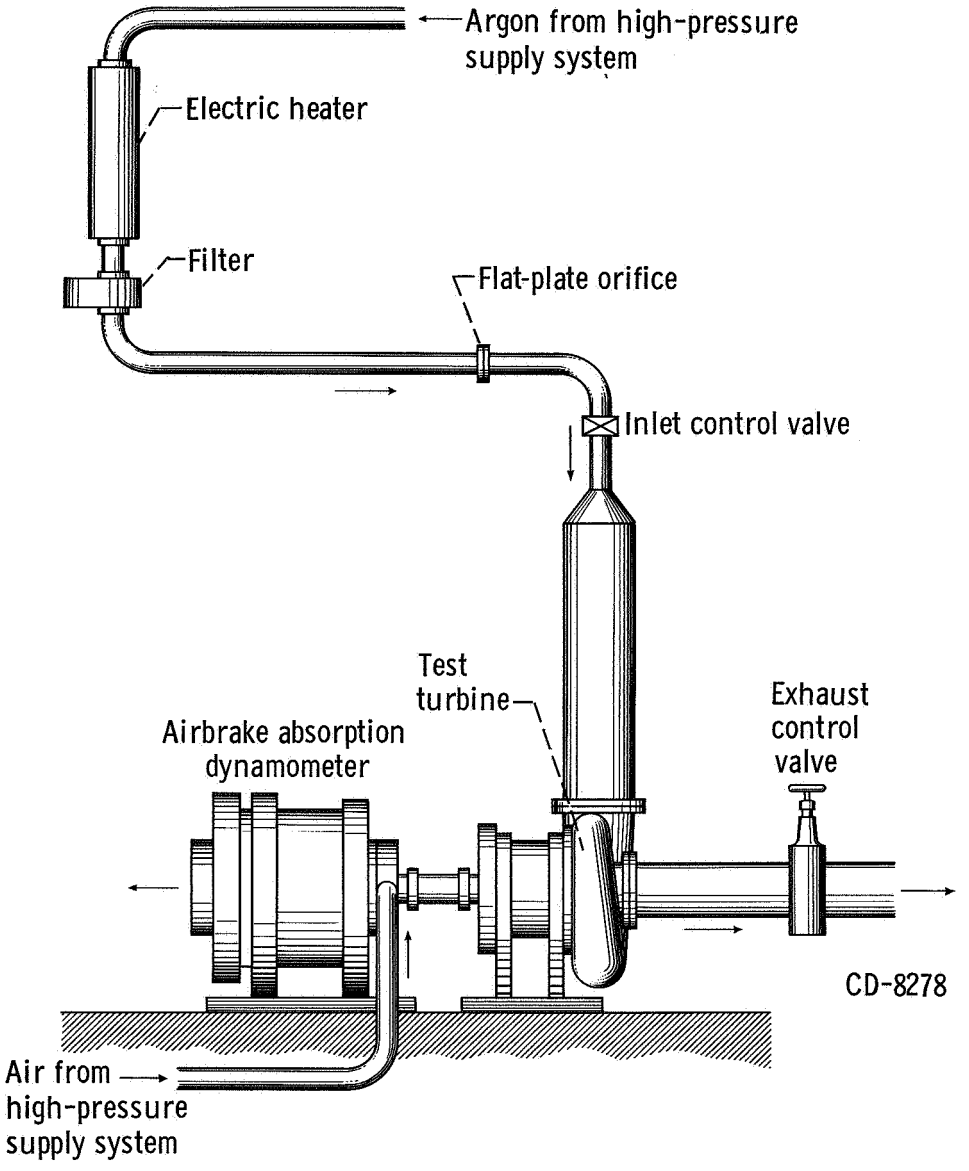

Figure 13. - Test apparatus.

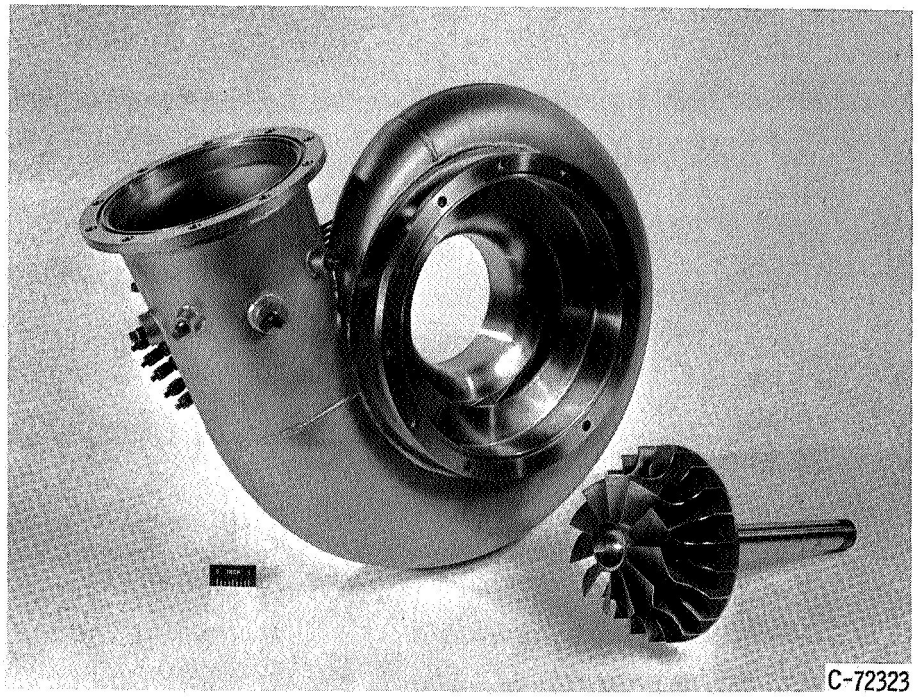

Figure 14. - 6.02-inch turbine rotor and scroll-stator assembly.

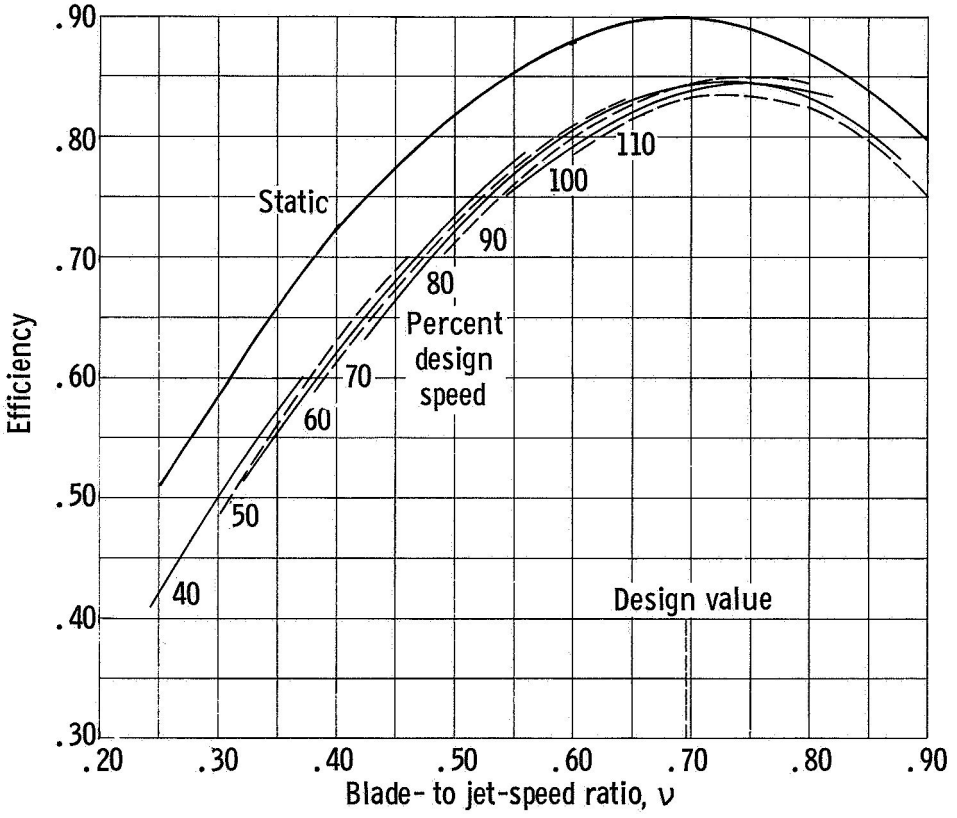

Figure 15. - Variation in efficiency with blade-jet speed ratio-6.02-inch turbine.

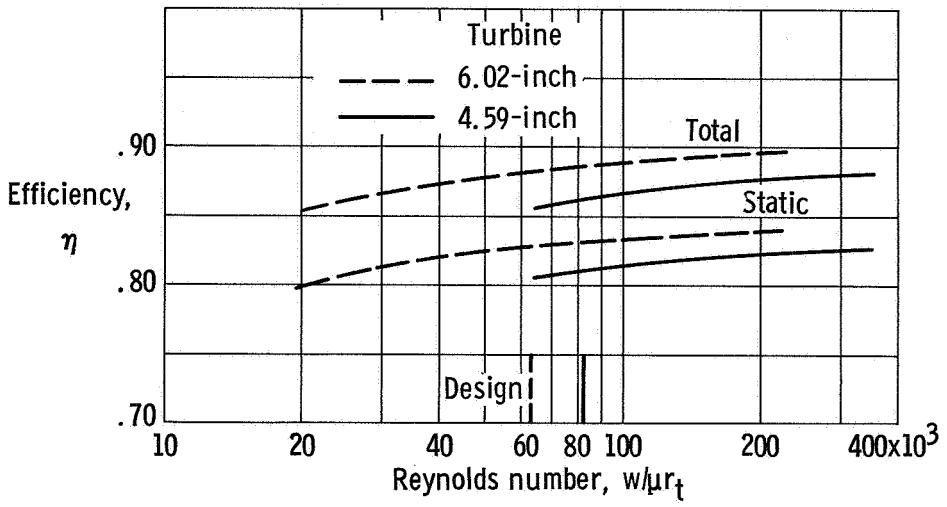

Figure 16. - Comparison of efficiency as function of Reynolds number at equivalent design speed and pressure ratio.

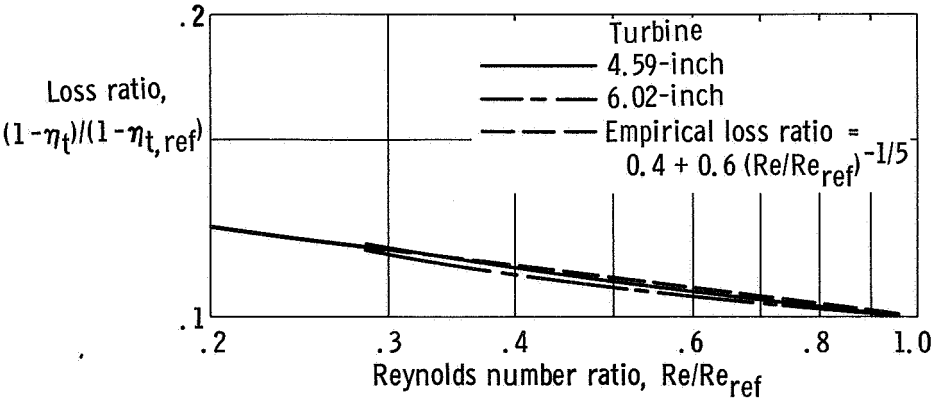

Figure 17. - Comparison of loss ratio as function of Reynolds number at equivalent design speed and pressure ratio.

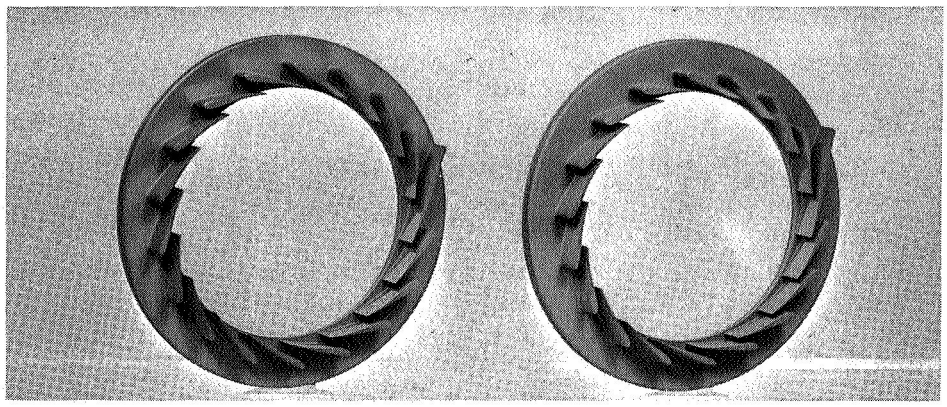

75 Percent design 50 Percent design

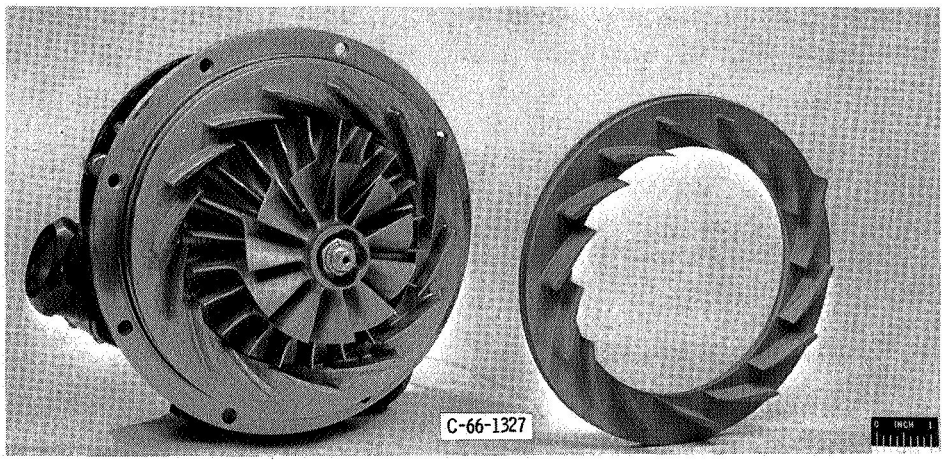

100 Percent design 125 Percent design

Figure 18. - Turbine rotor and four stators.

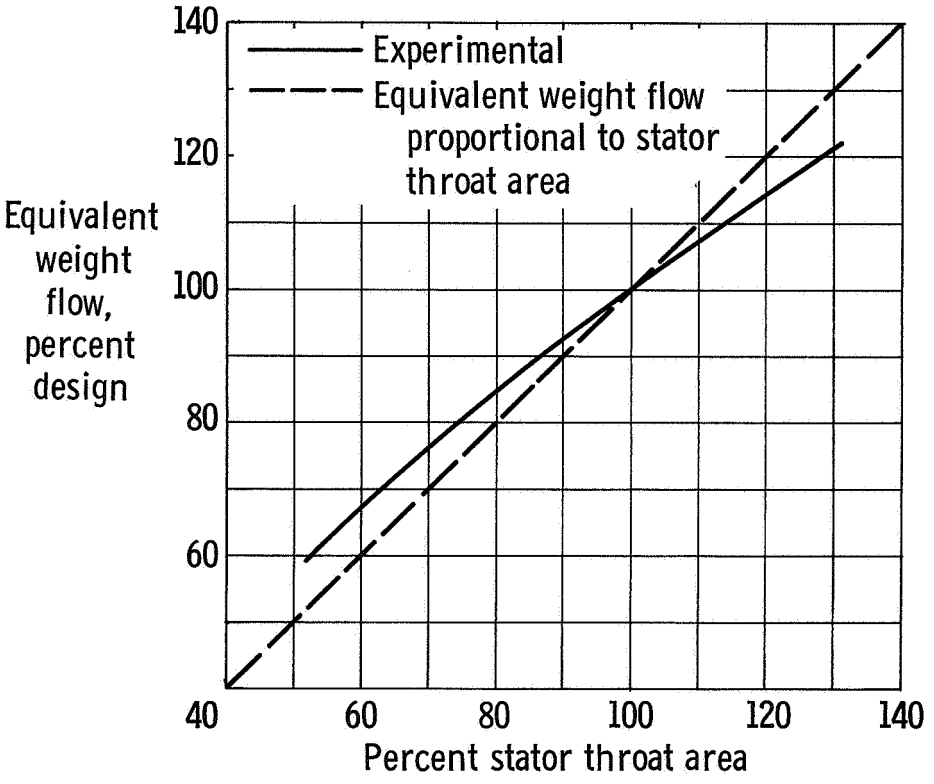

Figure 19. - Variation of weight flow with stator throat area at equivalent design speed and pressure ratio. (Based on measured throat area of 100-percent stator.) 4.59-inch turbine.

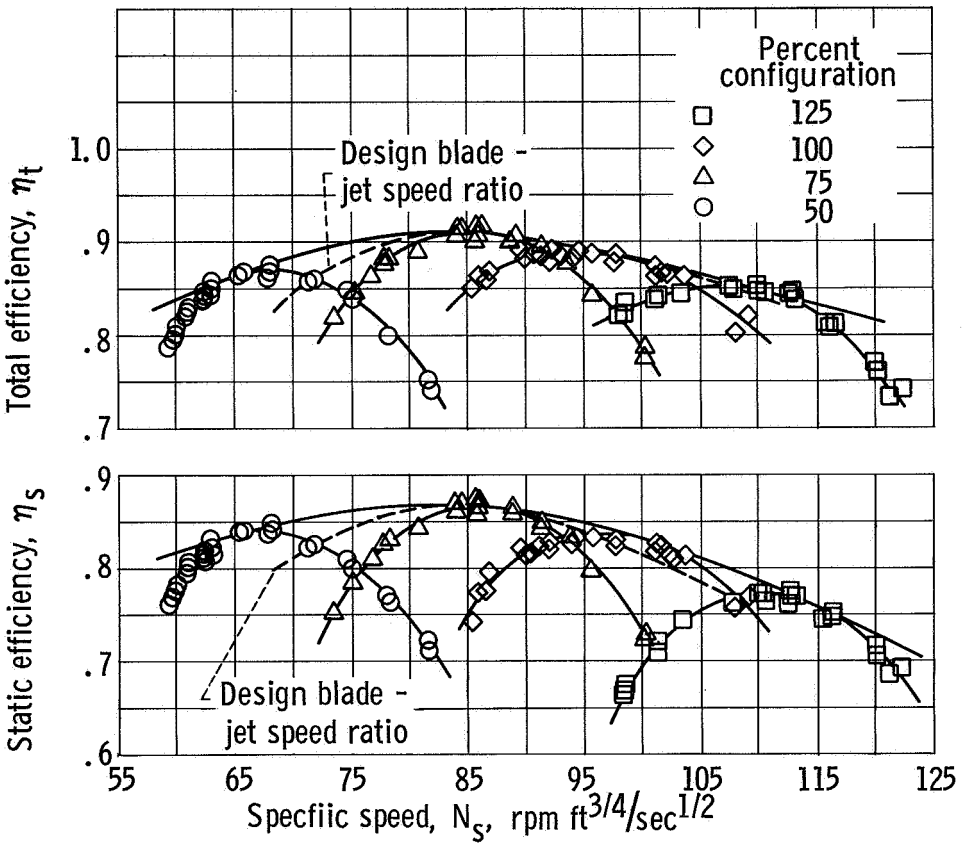

Figure 20. - Variation of efficiency with specific speed at equivalent design speed - 4.59-inch turbine.